Measurement of Spectral Correlation

WILLIAM A. GARDNER, SENIOR MEMBER, IEEE

Abstract—**Various methods for measurement/computation of spectral correlation functions for time series that exhibit cyclostationarity are described in a unifying theoretical framework. Some of these are amenable to digital hardware or software implementations, others are amenable to analog electrical or optical implementations, and other implementation types used for conventional spectral analysis are also possible. The interaction among reliability and temporal, spectral, and cycle resolutions is determined. Novel problems of computational complexity, cycle leakage and aliasing, cycle resolution, and cycle phasing are discussed. Sample spectral correlation functions are calculated with digital software for several simulated signals.**

GLOSSARY OF NOTATION

$\hat{R}_x^\alpha(\tau)$	Cyclic autocorrelation: (6), (11)
$R_{xT}^\alpha(t, \tau)$	Cyclic correlogram: (16) (T can be replaced with either Δt or $1/\Delta f$)
$\hat{S}_x^\alpha(f)$	Cyclic spectrum (spectral correlation function): (7), (8), (10)
$S_{xT}^\alpha(t, f)$	Cyclic periodogram: (14), (15) (T can be replaced with either Δt or $1/\Delta f$)
$S_{x\Delta t}^\alpha(t, f)_{\Delta f}$	Spectrally smoothed cyclic periodogram for continuous time: (18)
$S_{x1/\Delta f}^\alpha(t, f)_{\Delta t}$	Temporally smoothed cyclic periodogram for continuous time: (17)
$\tilde{S}_{x\Delta t}^\alpha(t, f)_{\Delta f}$	Spectrally smoothed cyclic periodogram for discrete time and frequency: (25)
$\tilde{S}_{x1/\Delta f}^\alpha(t, f)_{\Delta t}$	Temporally smoothed cyclic periodogram for discrete time and frequency: (26)
$X_T(t, f)$	Continuous-time complex envelope of narrow-band component of $x(t)$ with center frequency f and bandwidth $1/T$: (9) (T can be replaced with either Δt or $1/\Delta f$)
$\tilde{X}_T(t, f)$	Discrete-time complex envelope of narrow-band component of $x(t)$ with center frequency f and bandwidth $1/T$: (25b) (T can be replaced with either Δt or $1/\Delta f$)

I. INTRODUCTION

THE spectral analysis of stationary random time series has diverse applications in many fields of science and engineering. As a consequence, methods for improving resolution, reliability, and computational efficiency are prime subjects of research. However, many random time series encountered in the field of signal processing are more appropriately modeled as cyclostationary because of underlying periodicities due to various periodic signal processing operations such as sampling, scanning, modulating, multiplexing, and coding, or due to periodicity in the physical phenomenon that gives rise to the time series. These underlying periodicities are more subtle than the most commonly treated case of additive sine-wave components, and their properties are, in general, not reflected in the power spectral density function, which is a mean-square measure of spectral content. However, important characteristics of such underlying periodicity are reflected in the spectral correlation function. Although the spectral correlation function is equivalent to the set of cross-spectral densities for the set of all pairs of frequency-shifted versions of the time series, and cross-spectral analysis is an active area of research, there has been no focus, and in fact essentially no published work, on the problem of empirical spectral correlation analysis of cyclostationary time series. One reason for this is that analysts typically employ probabilistic models that incorporate a random phase variable that reduces the otherwise cyclostationary model to a stationary model, and stationary models exhibit no spectral correlation. A problem with this approach is that certain cycloergodic properties [1], [2] are destroyed by phase randomization in the sense that each sample path of such a process does indeed exhibit spectral correlation, but this correlation averages to zero over the ensemble of random phases in the probabilistic model.

The important role of spectral correlation analysis in the study of cyclostationary time series is discussed (within the probabilistic framework of stochastic processes) at some length in a chapter devoted to this subject in the book [1], where applications to detection, classification, parameter estimation, and extraction of cyclostationary signals, especially those buried in noise and further masked by interference, are discussed, and where an extensive set of examples of cyclostationary time series that arise in signal processing systems such as communications, radar, sonar, and telemetry, are described. In the simplest of terms, spectral correlation plays a fundamental role in any problem for which the cyclostationary autocorrelation function plays a central role, because the latter is completely characterized by the former. Specifically, the cyclostationary autocorrelation with period T_o is defined for a time series $x(t)$ by the average of lag products

Manuscript received April 23, 1985; revised April 22, 1986. This work was supported in part by ESL, a subsidiary of TRW.

The author is with the Department of Electrical and Computer Engineering, University of California, Davis, CA 95616.

IEEE Log Number 8609746.

$$\hat{R}_x(t, \tau) \triangleq \lim_{N\to\infty} \frac{1}{2N+1} \sum_{n=-N}^{N} x(t + nT_o + \tau/2) \cdot x(t + nT_o - \tau/2),$$
$$= \hat{R}_x(t + T_o, \tau), \quad (4)$$

which is synchronized to the period T_o. This periodic function can be expanded into a Fourier series,

$$\hat{R}_x(t, \tau) = \sum_{\alpha} \hat{R}_x^{\alpha}(\tau)\, e^{i2\pi\alpha t}, \quad (5)$$

where the Fourier coefficients are given by

$$\hat{R}_x^{\alpha}(\tau) \triangleq \frac{1}{T_o} \int_0^{T_o} \hat{R}_x(t, \tau)\, e^{-i2\pi\alpha t}\, dt \quad (6)$$

for α ranging over all integer multiples of the fundamental frequency of periodicity $1/T_o$. The Fourier transform of this lag-dependent coefficient,

$$\hat{S}_x^{\alpha}(f) = \int_{-\infty}^{\infty} \hat{R}_x^{\alpha}(\tau)\, e^{-i2\pi f\tau}\, d\tau, \quad (7)$$

is the spectral correlation function of interest for a given harmonic frequency α. Its interpretation as a spectral correlation function arises from the fact that it can be shown [1] that it is obtainable from the operations described by the expression

$$\hat{S}_x^{\alpha}(f) = \lim_{\Delta f\to 0} \lim_{\Delta t\to\infty} \frac{1}{\Delta t} \int_{-\Delta t/2}^{\Delta t/2} \Delta f X_{1/\Delta f}(t, f + \alpha/2) \cdot X_{1/\Delta f}^{*}(t, f - \alpha/2)\, dt, \quad (8)$$

where $X_{1/\Delta f}(t, \nu)$ is the complex envelope of the narrow-band-pass component of $x(t)$ with center frequency ν and approximate bandwidth Δf,

$$X_{1/\Delta f}(t, \nu) \triangleq \int_{t-1/2\Delta f}^{t+1/2\Delta f} x(u)\, e^{-i2\pi\nu u}\, du \quad (9)$$

(sometimes called the *short-time Fourier transform*). This expression (8) represents the limit, as spectral resolution becomes infinitesimal ($\Delta f \to 0$), of the limit ($\Delta t \to \infty$) temporal correlation of the two spectral components at frequencies $f + \alpha/2$ and $f - \alpha/2$. An introduction to the (nonprobabilistic) spectral correlation theory of cyclostationary time series is given in [3].

To see that the cyclostationary autocorrelation function plays a central role in many signal processing problems, one need only observe that the low-SNR likelihood ratio for detection and the low-SNR likelihood function for parameter estimation for a cyclostationary signal in additive noise is in general completely specified by the cyclostationary autocorrelation and the noise model (cf. [4] and [5].)

The purpose of this paper is to survey various alternative approaches to measurement of spectral correlation, within a unifying theoretical framework, and to bring to light the ways in which spectral correlation analysis of cyclostationary time series differs from conventional spectral analysis and cross-spectral analysis of stationary time series. For this purpose we begin with several alternative but equivalent definitions of the spectral correlation function (cf. [1] and [3].) In addition to the two definitions (4)–(7) and (8) and (9), it can be shown that $\hat{S}_x^{\alpha}(f)$ is given by the following limit of spectrally smoothed products of spectral components:

$$\hat{S}_x^{\alpha}(f) = \lim_{\Delta f\to 0} \lim_{\Delta t\to\infty} \frac{1}{\Delta f} \int_{f-\Delta f/2}^{f+\Delta f/2} \frac{1}{\Delta t} X_{\Delta t}(t, \nu + \alpha/2) \cdot X_{\Delta t}^{*}(t, \nu - \alpha/2)\, d\nu, \quad (10)$$

where $X_{\Delta t}(t, f)$ is defined by (9) with $1/\Delta f$ there replaced by Δt. It also can be shown[1] that (6) is given by the alternative formulas

$$\hat{R}_x^{\alpha}(\tau) = \lim_{\Delta t\to\infty} \frac{1}{\Delta t} \int_{-\Delta t/2}^{\Delta t/2} x(t + \tau/2)\, x(t - \tau/2)\, e^{-i2\pi\alpha t}\, dt, \quad (11)$$

and

$$\hat{R}_x^{\alpha}(\tau) = \lim_{\Delta t\to\infty} \frac{1}{\Delta t} \int_{-\Delta t/2}^{\Delta t/2} u(t + \tau/2)\, v^{*}(t - \tau/2)\, dt \quad (12)$$

where

$$u(t) = x(t)\, e^{-i\pi\alpha t} \quad (13)$$

$$v(t) = x(t)\, e^{+i\pi\alpha t}. \quad (14)$$

Consequently, $\hat{R}_x^{\alpha}(\tau)$ is the cross-correlation of $u(t)$ and $v(t)$, and it therefore follows from (7) that $\hat{S}_x^{\alpha}(f)$ is the cross-spectral density of $u(t)$ and $v(t)$. The function $\hat{R}_x^{\alpha}(\tau)$ given by (11) is called the *cyclic autocorrelation* and its Fourier transform $\hat{S}_x^{\alpha}(f)$, the spectral correlation function, is called the *cyclic spectral density*.

For convenience in the sequel, the integrand in definitions (8) and (10) is denoted by

$$S_{xT}^{\alpha}(t, f) = \frac{1}{T} X_T(t, f + \alpha/2)\, X_T^{*}(t, f - \alpha/2), \quad (14)$$

and is called the *cyclic periodogram*. The symbol T is used as a dummy parameter, which can represent either $T = 1/\Delta f$ as in (8) or $T = \Delta t$ as in (10). It can be shown that the cyclic periodogram is given by the Fourier transform

$$S_{xT}^{\alpha}(t, f) = \int_{-T}^{T} R_{xT}^{\alpha}(t, \tau)\, e^{-i2\pi f\tau}\, d\tau, \quad (15)$$

where the function

$$R_{xT}^{\alpha}(t, \tau) = \frac{1}{T} \int_{t-(T-|\tau|)/2}^{t+(T-|\tau|)/2} x(u + \tau/2) \cdot x(u - \tau/2)\, e^{-i2\pi\alpha u}\, du \quad (16)$$

[1] $\hat{R}_x^{\alpha}(\tau)$ given by (11) is the Fourier coefficient of the sine-wave component $e^{i2\pi\alpha t}$ contained in the lag product waveform $x(t + \tau/2)\, x(t - \tau/2)$, whereas $\hat{R}_x^{\alpha}(\tau)$ defined by (6) is the Fourier coefficient of $e^{i2\pi\alpha t}$ in $\hat{R}_x(t, \tau)$. Since $\hat{R}_x(t, \tau)$ as defined by (4) is simply the T_o-periodic component of $x(t + \tau/2)\, x(t - \tau/2)$, then these two Fourier components must be one and the same as long as α = integer/T_o. Furthermore, the equivalence of (11) and (12) follows directly from substitution of (13).

is called the *cyclic correlogram.* The parameters α and f are called the *cycle frequency* and *spectral frequency*, respectively.

It should be observed that for $\alpha = 0$, $\hat{R}_x^0(\tau)$ given by (11) is the conventional autocorrelation function, and $\hat{S}_x^0(f)$ given by (8) is the conventional power spectral density function, and (7) therefore reduces to the well-known Wiener relation for $\alpha = 0$ [1], [3]. Furthermore, for $\alpha = 0$, $S_{xT}^0(t, f)$ given by (14) and $R_{xT}^0(t, \tau)$ given by (16) are the conventional periodogram and correlogram, respectively. It should also be mentioned that if the time series $x(t)$ exhibits no cyclostationarity, then the autocorrelation in (4) is invariant to t, and the cyclic autocorrelation in (11) is identically zero for all $\alpha \neq 0$. Consequently, the spectral correlation function $\hat{S}_x^\alpha(f)$ is identically zero for all $\alpha \neq 0$ if the time series exhibits no cyclostationarity. This is particularly important for measurement of the spectral correlation of a signal masked by stationary noise, or for that matter masked by an interfering signal that does not exhibit cyclostationarity at the particular cycle frequencies of interest, because for sufficiently large values of $\Delta t \Delta f$ the effects of the masking noise or interference will be negligible (cf. Appendix B), and this is true regardless of spectral overlap between the signal of interest and the masking noise or interference. This potentially useful *noise-rejection* and *interference-rejection* property obviously does not exist for conventional spectral analysis ($\alpha = 0$).

As a final introductory remark, it is mentioned that if the time series $x(t)$ exhibits cyclostationarity with more than one period, and these periods are incommensurate, the representation (5) of the time-variant autocorrelation is still valid except that the sum ranges over all harmonics α of all the fundamental frequencies (reciprocal periods), as explained in [1] and [3]. In this case, the Fourier-coefficient functions in (5) are still given by (11), but no longer by (4) and (6).

In Section II of this paper, the interaction among reliability and temporal, spectral, and cycle resolutions of measured spectral correlation functions is briefly described. In Sections III–VII, a variety of methods for measurement of spectral correlation is described, and some of the novel problems associated with spectral correlation analysis are briefly discussed. In Section VIII, one of the digital methods implemented in software is used to provide samples of computed spectral correlation surfaces for several simulated signals.

II. Resolution and Reliability

It follows directly from definitions (8) and (10) that both the temporally smoothed cyclic periodogram [using $T = 1/\Delta f$ in (14)],

$$S_{x_{1/\Delta f}}^\alpha(t, f)_{\Delta t} \triangleq \frac{1}{\Delta t} \int_{t-\Delta t/2}^{t+\Delta t/2} S_{x_{1/\Delta f}}^\alpha(u, f)\, du, \qquad (17)$$

and the spectrally smoothed cyclic periodogram [using $T = \Delta t$ in (14)]

$$S_{x_{\Delta t}}^\alpha(t, f)_{\Delta f} \triangleq \frac{1}{\Delta f} \int_{f-\Delta f/2}^{f+\Delta f/2} S_{x_{\Delta t}}^\alpha(t, v)\, dv, \qquad (18)$$

provide estimates of the ideal spectral correlation function (which is obtained by letting $\Delta t \to \infty$ and then letting $\Delta f \to 0$). It is shown in Appendix A that these two estimates approximate each other for sufficiently large Δt ($\Delta t >> 1/\Delta f$). The rightmost subscript in (17) and (18) denotes both the type (temporal or spectral) and amount of smoothing. The *spectral resolution* capability of a measurement, such as (17) or (18), is the capability to resolve variational dependence on the spectral parameter f. The spectral resolution capability of the cyclic periodogram measurement $S_{xT}^\alpha(t, f)$ is denoted by Δf^o. Since the cyclic periodogram is defined by (14), then it follows that the spectral resolution capabilities of $S_{xT}^\alpha(t, f)$ and $X_T(t, f)$ are one and the same, and it follows from (9), as a well-known property of Fourier transformation, that the spectral resolution capability of $X_T(t, f)$ is on the order of the reciprocal $1/T$ of the length of the waveform segment that is Fourier transformed

$$\Delta f^o \cong 1/T. \qquad (19)$$

Also, since $X_T(t, f)$, and therefore, $S_{xT}^\alpha(t, f)$ is obtained by integration in time over a sliding interval of length T, then the *temporal resolution* capability, denoted by Δt^o, of $S_{xT}^\alpha(t, f)$ is simply

$$\Delta t^o = T. \qquad (20)$$

Thus, the temporal-spectral resolution product is approximately unity,

$$\Delta t^o \Delta f^o \cong 1 \qquad (21)$$

regardless of the value of T. Now, when the cyclic periodogram is smoothed as in (17) or (18), then one of these two resolution capabilities is decreased. In order to obtain a substantial reduction in random effects, it is required that a substantial amount of smoothing be used. Thus, for (17) it is required that

$$\Delta t >> 1/\Delta f = T$$

and for (18) it is required that

$$\Delta f >> 1/\Delta t = 1/T.$$

In (17), the temporal smoothing operation increases the temporal resolution width from $\Delta t^o = T = 1/\Delta f$ to $\Delta t >> 1/\Delta f$, and in (18), the spectral smoothing operation increases the spectral resolution width from $\Delta f^o = 1/T = 1/\Delta t$ to $\Delta f >> 1/\Delta t$. Thus, for both estimates (17) and (18), the temporal-spectral resolution product must greatly exceed unity

$$\Delta t \Delta f >> 1 \qquad (22)$$

in order to obtain a substantial reduction in random effects. This is a well-known result for conventional spectral analysis ($\alpha = 0$), which is sometimes referred to as *Grenander's uncertainty condition* for reliable spectrum estimation, and can be similarly corroborated for spectral

correlation analysis by mathematical analysis of the temporal mean and temporal variance of the spectral correlation estimates, as shown in Appendix B. For example, for $\Delta t \Delta f >> 1$, and Δf small enough to resolve the spectral correlation function, it is shown in Appendix B that the temporal variance normalized by the squared temporal mean is typically dominated by a term that is approximately $1/\Delta t \Delta f$ divided by the autocoherence function magnitude

$$|\hat{C}_x^\alpha(f)| \triangleq \frac{|\hat{S}_x^\alpha(f)|}{[\hat{S}_x^0(f + \alpha/2)\, \hat{S}_x^0(f - \alpha/2)]^{1/2}}$$

for a time series with Gaussian fraction-of-time distribution.

A cyclic spectrum estimate is said to be *reliable* only if the random effects have been made sufficiently small, in which case the spectrum estimate is nearly independent of the time t at which it is measured (ideally for all $|t| < \infty$). Consequently, (22) reveals that there is a fundamental tradeoff among temporal resolution, spectral resolution, and reliability. This is a well-known fact for conventional spectral analysis ($\alpha = 0$). For spectral correlation analysis, however, there is yet another resolution parameter involved, namely, the *cycle resolution* denoted by $\Delta\alpha$. It is shown in Appendices A and B that, for both estimates (17) and (18), $\Delta\alpha$ is on the order of $1/\Delta t$

$$\Delta\alpha = 1/\Delta t, \tag{23}$$

regardless of the value of Δf. That is, these estimates cannot resolve spectral correlation for two cycle frequencies unless these frequencies are separated by more than $\Delta\alpha = 1/\Delta t$. Thus, the *reliability condition* (22) can be reexpressed as

$$\Delta f/\Delta\alpha >> 1, \tag{24}$$

i.e., the resolution in α must be much finer than the resolution in f for high reliability. Although this result can be exploited in certain applications, it can also be a source of problems for implementation as discussed in Section III, and in more detail in [6].

It should be clarified that temporal resolution is of interest when spectral correlation is a local phenomena that changes with time and therefore requires a tracking measurement. When spectral correlation does not change with time (for practical purposes), the temporal resolution Δt simply denotes the total *integration time* which is approximately equal to the total amount of data used in the measurement.

Another performance characteristic that is as important as resolution and reliability is leakage. The *cycle leakage* and *spectral leakage* effects associated with resolution are quantified in the following section and Appendix B.

III. Methods Based on the Cyclic Periodogram

One feasible approach to implementation of the two cyclic spectrum estimates (17) and (18), obtained by temporally or spectrally smoothing the cyclic periodogram, is based on digital implementations that use the FFT algorithm for computation of a discrete-time/discrete-frequency counterpart of the sliding-window complex Fourier transform (9). However, analog electrical filtering methods may be needed for large bandwidths, and optical implementations also appear to be feasible for some applications, and perhaps preferred for large bandwidths. For digital implementation, computational complexity can be a cruical issue, especially when a full cyclic spectral analysis (spectral correlation analysis) over a broad range of both f and α is desired. The development of computationally efficient algorithms for cyclic spectral analysis is a current topic of research. Only the two most straightforward smoothing methods are mentioned here.

The discrete-frequency smoothing method is given by

$$\tilde{S}_{x\Delta t}^\alpha(t, f)_{\Delta f} = \frac{1}{M} \sum_{v=-(M-1)/2}^{(M-1)/2} \frac{1}{\Delta t} \tilde{X}_{\Delta t}(t, f + \alpha/2 + vF_s)\, \tilde{X}_{\Delta t}^*(t, f - \alpha/2 + vF_s), \tag{25a}$$

where

$$\tilde{X}_{\Delta t}(t, f) \triangleq \sum_{k=0}^{N-1} a_{\Delta t}(kT_s)\, x(t - kT_s)\, e^{-i2\pi f(t - kT_s)}, \tag{25b}$$

which is the downconverted output of a sliding DFT, and where $a_{\Delta t}$ is the data-tapering window, $\Delta f = MF_s$ is the width of the spectral smoothing interval, $F_s = 1/NT_s$ is the frequency sampling increment, T_s is the time-sampling increment, and N is the number of time samples in the data segment of length Δt, which is Fourier transformed by the DFT, $N = \Delta t/T_s + 1$. Thus, the resolution product is $\Delta t \Delta f = M(N - 1)/N \cong M$.

The discrete-time averaging method is given by

$$\tilde{S}_{x1/\Delta f}^\alpha(t, f)_{\Delta t} = \frac{1}{KM} \sum_{u=0}^{KM-1} \Delta f \tilde{X}_{1/\Delta f}(t - u/K\Delta f, f + \alpha/2) \cdot \tilde{X}_{1/\Delta f}^*(t - u/K\Delta f, f - \alpha/2), \tag{26}$$

where $\tilde{X}_{1/\Delta f}(t, f)$ is the downconverted output of a sliding DFT, and where $\Delta t = ([1 + M - 1/K]N - 1)\, T_s$ is the length of the total data segment, $\Delta f = 1/(N - 1)\, T_s$ is the spectral resolution, and N is the number of time samples in each of the data segments of length $1/\Delta f$, which are Fourier transformed by the DFT. Thus, the resolution product is $\Delta t \Delta f = ([1 + M - 1/K]N - 1)/(N - 1) \cong M$. Because of a *cycle leakage* phenomenon that does not occur for conventional spectral analysis of stationary data, the block-overlap parameter K, in (26), often cannot be taken as small (e.g., $K = 1$ or 2) as it is for the conventional hopping-FFT method for spectral analysis. Detailed analysis, based on (28), and simulations reveal that $K = 4$ is typically the minimum tolerable value when properly designed data-tapering apertures are used. However, the actual value of K required depends on the strength of cycles present in the data. This is clarified in the following paragraph. Another phenomenon that does not occur for conventional spectral analysis is the decrease in cycle resolution width, $\Delta\alpha = 1/\Delta t$, with an in-

crease in the number KM of blocks averaged. In fact, $\Delta\alpha = \Delta f(N-1)/([1+M-1/K]N-1) \cong \Delta f/M$ is inversely proportional to the effective number M of nonoverlapping blocks. However, the frequency sampling increment provided by the FFT used to transform each block is $F_s = 1/NT_s \cong \Delta f$, which does not decrease as $\Delta\alpha$ decreases. Thus, adjacent cycle frequency samples are separated by $F_s/\Delta\alpha = M$ cycle resolution widths. Consequently, the density of cycle frequency samples is $1/M$ times what it should be in order not to miss parts of the cyclic spectrum. This is especially problematic because the cyclic spectrum is, by nature, discrete in α [1]. An obvious but computationally burdensome remedy is to zero-pad the blocks of length N out to length MN to obtain a frequency sampling increment of $F_s = \Delta f/M$. More sophisticated remedies that are substantially more computationally efficient for large N are currently being developed [6].

Cycle Leakage: The discrete-time averaging (hopping-FFT) method of cyclic spectrum analysis effectively employs an output comb filter, rather than an output low-pass filter, and this can result in cycle leakage. Unfortunately, as the amount of overlap between adjacent blocks is decreased (K decreased) to improve computational efficiency, the effects of the cycle leakage phenomenon worsen. This can be illustrated for continuous time as well as for discrete time. For example, the statistical cyclic spectrum

$$S^{\alpha}_{xT}(t,f)_{\Delta t} \triangleq \frac{1}{L}\sum_{u=-(L-1)/2}^{(L-1)/2} S^{\alpha}_{xT}(t+uT/K,f) \tag{27}$$

obtained by advancing the temporal index by integer multiples of T/K to cover a total time span of approximately $\Delta t = LT/K$, can be expressed as the sum of its temporal mean (cf. Appendix B) and a residual,

$$S^{\alpha}_{xT}(t,f) = \sum_{\beta}\left\{\hat{S}^{\beta}_{x}(f) \otimes \left[\frac{1}{T}A_{1/T}(f+[\beta-\alpha]/2) \cdot A^{*}_{1/T}(f-[\beta-\alpha]/2)\right]\right\} C_{K/LT}(\beta-\alpha)\, e^{i2\pi(\beta-\alpha)t} + \text{residual}, \tag{28}$$

where

$$C_{K/LT}(f) \triangleq \sum_{m=-\infty}^{\infty} w_{K/LT}(f-mK/T), \tag{29}$$

and the residual converges to zero as $L \to \infty$. In (28), $\otimes$ denotes convolution with respect to the variable f, $A_{1/T}$ is the Fourier transform of the data-tapering aperture a_T used in $S^{\alpha}_{xT}(t,f)$ [e.g., a_T is a rectangle in (9)], and the sum is over all β for which $\hat{S}^{\beta}_{x}(f) \not\equiv 0$. In (29), w_{Δ} is a unity-height sinc window with null-to-null width 2Δ. It follows from (28) that in addition to the desired cyclic line which shows up if $\alpha = \beta$ for some cycle-frequency β contained in $x(t)$, additional lines show up due to other cycle frequencies, $\beta \neq \alpha$ (including $\beta = 0$) contained in $x(t)$, for which the *cycle-smoothing comb-window* (29), and the *spectral-smoothing product window*

$$\frac{1}{T}A_{1/T}(f+[\beta-\alpha]/2)\, A^{*}_{1/T}(f-[\beta-\alpha]/2), \tag{30}$$

are both sufficiently large to pass the cyclic contribution from $\hat{S}^{\beta}_{x}(f)$. These undesired contributions that leak through the windows can be made as small as desired by selecting K sufficiently large to render the separation between cycles passed by adjacent teeth of the comb window sufficiently large, designing the data-tapering aperture to render the sidelobes of the product window sufficiently low, and choosing LT sufficiently large. This can be seen from the fact that the comb window has teeth, with width parameter K/LT, separated by integer multiples of K/T. Thus, K must be large enough to render the window product

$$\frac{1}{T}A_{1/T}(f+mK/2T)\, A^{*}_{1/T}(f-mK/2T) \tag{31}$$

that coincides with the mth tooth of the comb window sufficiently small for all nonzero integers m. Of course, leakage will occur only if there are cycles present at appropriate frequencies; that is, potential leakage requires $|\beta-\alpha-mK/T| < K/LT$ for those values of β for which $\hat{S}^{\beta}_{x}(f) \not\equiv 0$.

IV. Fourier Transformation of Tapered Cyclic Autocorrelation or Ambiguity Function

Application of the convolution theorem and the cyclic-periodogram/cyclic-correlogram relation [(15)] to (18) reveals that a spectrally smoothed cyclic periodogram can be obtained by Fourier transformation of a tapered cyclic correlogram

$$S^{\alpha}_{x\Delta t}(t,\cdot)_{\Delta f} \triangleq S^{\alpha}_{x\Delta t}(t,\cdot) \otimes H_{\Delta f}(\cdot) = F\{R^{\alpha}_{x\Delta t}(t,\cdot)\, h_{1/\Delta f}(\cdot)\} \tag{32a}$$

where

$$R^{\alpha}_{x\Delta t}(t,\tau) \triangleq \frac{1}{\Delta t}\int_{t-(\Delta t-|\tau|)/2}^{t+(\Delta t-|\tau|)/2} x(u+\tau/2) \cdot x(u-\tau/2)\, e^{-i2\pi\alpha u}\, du, \tag{32b}$$

$$h_{1/\Delta f}(\cdot) \triangleq F^{-1}\{H_{\Delta f}(\cdot)\}, \tag{32c}$$

and $F^{-1}\{\cdot\}$ denotes inverse Fourier transformation, and $H_{\Delta f}$ is the spectral smoothing window [e.g., $H_{\Delta f}$ is a rectangle in (18)]. Since considerable effort has gone into the development of methods for measurement/computation of radar ambiguity functions, it should be mentioned that the cyclic correlogram in (32) can be reinterpreted as an ambiguity function (cf. [1] and [3]), and therefore, some knowledge and methods (e.g., for optical implementations [7]–[14]) can be transferred from the radar ambiguity problem area to the cyclic spectral analysis area, although caution must be used here because of the distinct differences between the radar ambiguity function for the complex envelope of a time series and the ambiguity function (cyclic correlogram) for the real-time series.

V. Fourier Transformation of Spectrally Smoothed Wigner–Ville Distribution

It can be shown that the cyclic periodogram is the normalized (by Δt) Fourier transform of the Wigner–Ville distribution [15] of the finite data segment[2] of length Δt

$$y(t) \triangleq x(t)\, u_{\Delta t}(t' - t).$$

That is,

$$S^{\alpha}_{x_{\Delta t}}(t', f) = \frac{1}{\Delta t} \int_{-\infty}^{\infty} E_y(t, f)\, e^{-i2\pi\alpha t}\, dt, \tag{33}$$

in which the dependence of the Wigner–Ville distribution $E_y(t, f)$ on the location t' of the segment y of x is suppressed in the notation

$$E_y(t, f) \triangleq \int_{-\infty}^{\infty} y(t + \tau/2)\, y(t - \tau/2)\, e^{-i2\pi f\tau}\, d\tau. \tag{34}$$

Therefore, the spectrally smoothed cyclic spectrum can be obtained from the spectrally smoothed Wigner–Ville distribution by Fourier transformation

$$S_{x_{\Delta t}}(t', f)_{\Delta f} \triangleq S^{\alpha}_{x_{\Delta t}}(t', f) \otimes H_{\Delta f}(f) = \frac{1}{\Delta t} \int_{-\infty}^{\infty} [E_y(t, f) \otimes H_{\Delta f}(f)]\, e^{-i2\pi\alpha t}\, dt. \tag{35}$$

Furthermore, the spectrally smoothed Wigner–Ville distribution can be obtained by lag-product tapering

$$E_y(t, f) \otimes H_{\Delta f}(f) = \int_{-\infty}^{\infty} y(t + \tau/2)\, y(t - \tau/2)\, h_{1/\Delta f}(\tau)\, e^{-i2\pi f\tau}\, d\tau. \tag{36}$$

It follows from (35) and (36) that methods of implementation, such as acoustooptical methods for broad-band analysis [7]–[14], which have been developed for measurement of the Wigner–Ville distribution [16], are potentially useful for measurement of the cyclic spectrum.

VI. Cyclic Wave Analysis

The temporally smoothed cyclic periodogram (17), generalized for tapered data by use of

$$X_T(t, \nu) = \int_{-\infty}^{\infty} a_T(t - u)\, x(u)\, e^{-i2\pi\nu u}\, du,$$

in place of (9), can be reexpressed (by executing a low-pass-to-band-pass transformation) as

$$S^{\alpha}_{x_{1/\Delta f}}(t, f)_{\Delta t} = \Delta f\{[x(t)\, e^{-i\pi\alpha t} \otimes a^{f}_{1/\Delta f}(t)] \cdot [x(t)\, e^{i\pi\alpha t} \otimes a^{f}_{1/\Delta f}(t)]^*\} \otimes g_{\Delta t}(t), \tag{37a}$$

in which

$$a^{f}_{1/\Delta f}(t) \triangleq a_{1/\Delta f}(t)\, e^{i2\pi f t}, \tag{37b}$$

where $a_{1/\Delta f}$ is the data-tapering aperture, $g_{\Delta t}$ is the temporal smoothing window, and the convolution is with respect to the variable t. Formula (37) can be reexpressed (by executing a band-pass-to-band-pass transformation) as

[2]The symbol $u_{\Delta t}$ denotes a unity-height rectangle of width Δt.

$$S^{\alpha}_{x_{1/\Delta f}}(t, f)_{\Delta t} = \Delta f(\{[x(t) \otimes a^{\alpha/2+f}_{1/\Delta f}(t)] \cdot [x(t) \otimes a^{\alpha/2-f}_{1/\Delta f}(t)]\} \otimes g^{\alpha}_{\Delta t}(t))\, e^{-i2\pi\alpha t}, \tag{38a}$$

in which

$$a^{\alpha/2\pm f}_{1/\Delta f}(t) \triangleq a_{1/\Delta f}(t)\, e^{i2\pi(\alpha/2 \pm f)t} \tag{38b}$$

$$g^{\alpha}_{\Delta t}(t) \triangleq g_{\Delta t}(t)\, e^{i2\pi\alpha t}. \tag{38c}$$

The smoothing functions defined by (38b) and (38c) can be interpreted as the impulse-response functions of filters with transfer functions

$$A^{\alpha/2\pm f}_{\Delta f}(\nu) = A_{\Delta f}(\nu - \alpha/2 \mp f) \tag{39a}$$

$$G^{\alpha}_{1/\Delta t}(\nu) = G_{1/\Delta t}(\nu - \alpha), \tag{39b}$$

where

$$A_{\Delta f}(\cdot) \triangleq F\{a_{1/\Delta f}(\cdot)\} \tag{39c}$$

$$G_{1/\Delta t}(\cdot) \triangleq F\{g_{\Delta t}(\cdot)\}. \tag{39d}$$

Thus, $A^{\alpha/2\pm f}_{\Delta f}$ and $G^{\alpha}_{1/\Delta t}$ are the transfer functions of one-sided (i.e., complex) BPF's (band-pass filters) with center frequencies $\alpha/2 \pm f$ and α, respectively, and with bandwidths Δf and $1/\Delta t$, respectively. Formula (38a), therefore, reveals that the temporally smoothed cyclic spectrum $S^{\alpha}_{x_{1/\Delta f}}(t, f)_{\Delta t}$ can be obtained by filtering $x(t)$ with two complex BPF's, multiplying the results, filtering the product with a complex BPF, and then frequency shifting the result down by α to the vicinity of zero frequency, as depicted in Fig. 1(a). By analogy with the term *wave analysis* used for conventional spectral analysis ($\alpha = 0$), this method for cyclic spectrum analysis shall be called *cyclic wave analysis*.

In order to obtain a real implementation, the real part of $S^{\alpha}_{x_{1/\Delta f}}(t, f)_{\Delta t}\, e^{i2\pi\alpha t}$, from (38a), is taken to obtain

$$\begin{aligned}
&[S^{\alpha}_{x_{1/\Delta f}}(t, f)_{\Delta t}\, e^{i2\pi\alpha t}]_r \\
&\quad = |S^{\alpha}_{x_{1/\Delta f}}(t, f)_{\Delta t}| \cos(2\pi\alpha t + \arg\{S^{\alpha}_{x_{1/\Delta f}}(t, f)_{\Delta t}\}) \\
&\quad = (\{x(t) \otimes [a_{1/\Delta f}(t) \cos(2\pi[\alpha/2 + f]t)]\} \\
&\qquad \cdot \{x(t) \otimes [a_{1/\Delta f}(t) \cos(2\pi[\alpha/2 - f]t)]\} \\
&\qquad - \{x(t) \otimes [a_{1/\Delta f}(t) \sin(2\pi[\alpha/2 + f]t)]\} \\
&\qquad \cdot \{x(t) \otimes [a_{1/\Delta f}(t) \sin(2\pi[\alpha/2 - f]t)]\}) \\
&\qquad \otimes [g_{\Delta t}(t) \cos(2\pi\alpha t)] \\
&\qquad - (\{x(t) \otimes [a_{1/\Delta f}(t) \cos(2\pi[\alpha/2 + f]t)]\} \\
&\qquad \{x(t) \otimes [a_{1/\Delta f}(t) \sin(2\pi[\alpha/2 - f]t)]\} \\
&\qquad + \{x(t) \otimes [a_{1/\Delta f}(t) \cos(2\pi[\alpha/2 - f]t)]\} \\
&\qquad \{x(t) \otimes [a_{1/\Delta f}(t) \sin(2\pi[\alpha/2 + f]t)]\}) \\
&\qquad \otimes [g_{\Delta t}(t) \sin(2\pi\alpha t)].
\end{aligned} \tag{40}$$

Formula (40) can be implemented as shown in Fig. 1(b). Thus, a real implementation of the cyclic wave analyzer

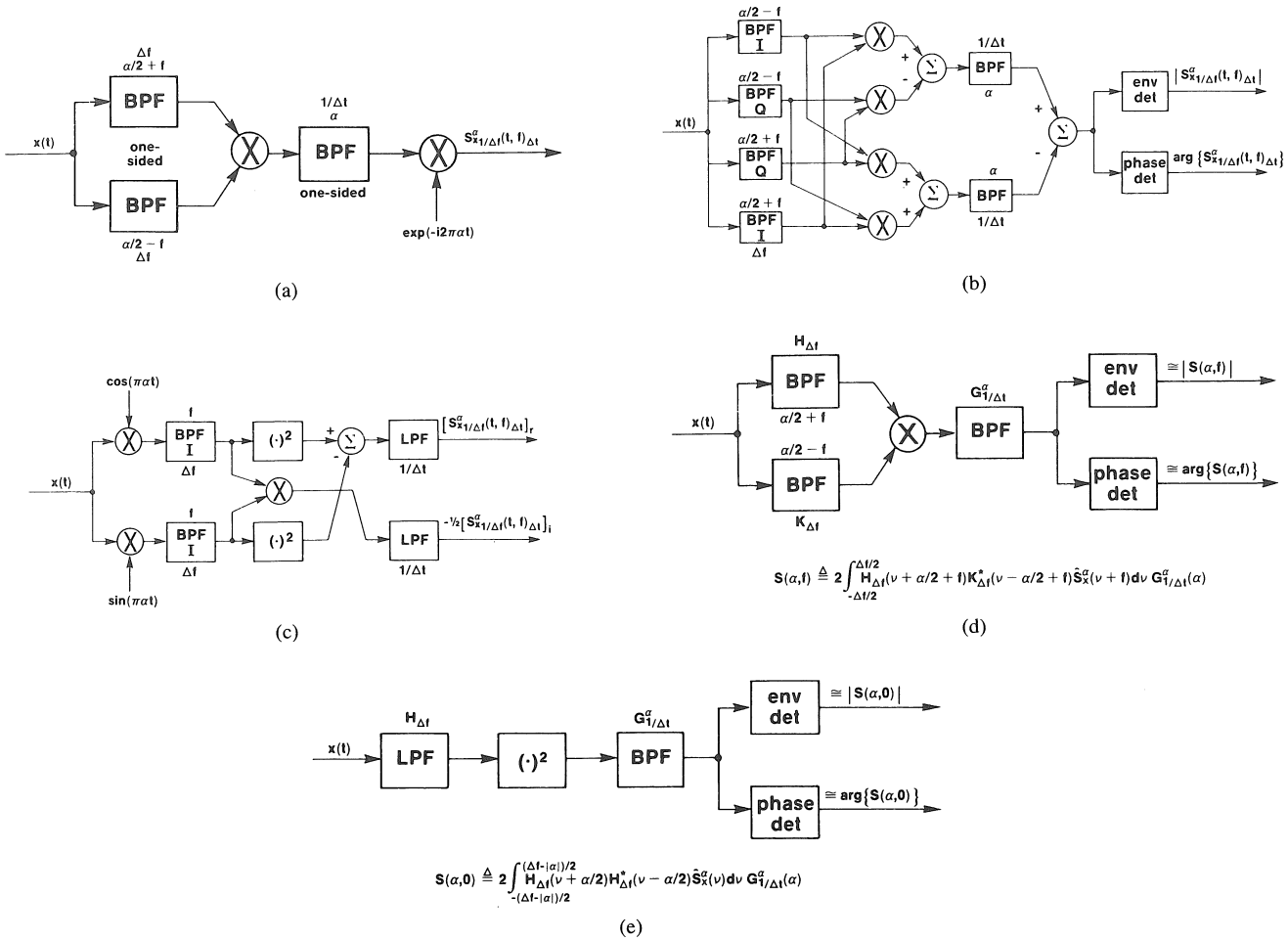

Fig. 1. (a) Complex implementation of cyclic wave analyzer. (b) Real implementation number 1 of cyclic wave analyzer. (c) Real implementation number 2 of cyclic wave analyzer. (d) Real implementation number 3 of cyclic wave analyzer. (Input BPF's satisfy the condition $|\alpha/2 \pm f| > \Delta f/2$.) (e) Real implementation number 4 of cyclic wave analyzer. (Input LPF satisfies $|\alpha| < \Delta f$.)

is quite complicated since it requires six special symmetric BPF's, four multipliers, and three adders. It should be mentioned at this point that a quadrature BPF (Q-BPF), with impulse response

$$a(t) \sin (2\pi\nu t),$$

can be obtained from an in-phase BPF (I-BPF), with impulse response

$$a(t) \cos (2\pi\nu t),$$

by following (or preceding) the I-BPF with a Hilbert transforming filter. This equivalence is exact as long as $a(t)$ is band-limited to $f \in (-\nu, \nu)$ [1].

Another approach to obtaining a real implementation is to substitute the representation

$$x(t)\, e^{\pm i\pi\alpha t} = c(t) \pm is(t), \tag{41a}$$

where

$$c(t) \triangleq x(t) \cos (\pi\alpha t) \tag{41b}$$

$$s(t) \triangleq x(t) \sin (\pi\alpha t), \tag{41c}$$

into (37a) to obtain the real and imaginary parts

$$[S^{\alpha}_{x1/\Delta f}(t, f)_{\Delta t}]_r = S_{c1/\Delta f}(t, f)_{\Delta t} - S_{s1/\Delta f}(t, f)_{\Delta t} \tag{42a}$$

$$\begin{aligned}[S^{\alpha}_{x1/\Delta f}(t, f)_{\Delta t}]_i &= -[S_{cs1/\Delta f}(t, f)_{\Delta t} + S_{sc1/\Delta f}(t, f)_{\Delta t}] \\ &= -2[S_{cs1/\Delta f}(t, f)_{\Delta t}]_r,\end{aligned} \tag{42b}$$

in which the terms in the right members are conventional spectrum estimates such as

$$S_{cs1/\Delta f}(t, f)_{\Delta t} = \Delta f \{[c(t) \otimes a^{f}_{1/\Delta f}(t)][s(t) \otimes a^{f}_{1/\Delta f}(t)]^*\} \otimes g_{\Delta t}(t). \tag{42c}$$

As is well known, the wave analysis method of cross-spectral analysis requires special symmetric filters. Thus, this alternative real implementation is still somewhat complicated, as shown in Fig. 1(c), but simpler than that shown in Fig. 1(b). Nevertheless, the characterization (42) of the spectral correlation estimate is revealing. In particular, it is typically assumed for conventional spectral analysis that both (42a) and (42b) are negligible compared to $S_{x1/\Delta f}(t, f)_{\Delta t}$ for $\Delta t \Delta f >> 1$. It is quite clear from (42)

that this assumption is valid (for $\Delta t \Delta f >> 1$) for all α if and only if $x(t)$ exhibits no cyclostationarity.

Yet another approach to obtaining real implementations is based on the representation[3]

$$S^{\alpha}_{x_{1/\Delta f}}(t, f)'_{\Delta t} \triangleq \{[x(t) \otimes h_{1/\Delta f}(t)][x(t) \otimes k_{1/\Delta f}(t)]\} \otimes g^{\alpha}_{\Delta t}(t) \quad (43a)$$

$$= \text{Re}\left\{\left[\int_{-\infty}^{\infty} H_{\Delta f}(\alpha/2 + \nu)\, K_{\Delta f}(\alpha/2 - \nu) \cdot \hat{S}^{\alpha}_{x}(\nu)\, d\nu\right][G^{\alpha}_{1/\Delta t}(\alpha)\, e^{i2\pi\alpha t}]\right\} + \text{residual}, \quad \Delta t \Delta f >> 1, \quad (43b)$$

in which the residual becomes increasingly negligible as $\Delta t \Delta f \to \infty$ for any fixed Δf. In (43b), $H_{\Delta f}$ and $K_{\Delta f}$ are the transfer functions of two arbitrary filters with bandwidths of Δf,

$$H_{\Delta f}(\cdot) = F\{h_{1/\Delta f}(\cdot)\} \quad (44a)$$

$$K_{\Delta f}(\cdot) = F\{k_{1/\Delta f}(\cdot)\}, \quad (44b)$$

and $G^{\alpha}_{1/\Delta t}$ is the transfer function of an arbitrary BPF with center frequency α, and bandwidth $1/\Delta t$,

$$G^{\alpha}_{1/\Delta t}(\cdot) = F\{g^{\alpha}_{\Delta t}(\cdot)\}. \quad (44c)$$

The first term in the right member of (43b) is the temporal mean of the left member (cf. Appendix B). There are two cases of interest identified by the relative magnitudes of the smoothing bandwidth Δf and the frequencies $|\alpha|/2 \pm |f|$.

Case 1: It can be shown that if $H_{\Delta f}$ is a BPF with center frequency $\alpha/2 + f$, and $K_{\Delta f}$ is a BPF with center frequency $\alpha/2 - f$, and if

$$|f \pm \alpha/2| > \Delta f/2, \quad (45)$$

then (43) reduces to

$$S^{\alpha}_{x_{1/\Delta f}}(t, f)'_{\Delta t} = |S(\alpha, f)| \cos(2\pi\alpha t + \arg\{S(\alpha, f)\}) + \text{residual}, \quad (46a)$$

in which

$$S(\alpha, f) \triangleq 2 \int_{-\Delta f/2}^{\Delta f/2} H_{\Delta f}(\nu + \alpha/2 + f) \cdot K_{\Delta f}(-\nu + \alpha/2 - f)\, \hat{S}^{\alpha}_{x}(\nu + f)\, d\nu\, G^{\alpha}_{1/\Delta t}(\alpha). \quad (46b)$$

Thus, an envelope detector at the output of the real quadratic time-invariant device represented by (43a) yields the magnitude of the spectrally smoothed cyclic spectrum (46b) as depicted in Fig. 1(d). The difficulty with this approach, however, is the problem of designing tunable BPF's $H_{\Delta f}$ and $K_{\Delta f}$ with appropriate phase characteristics. For example, to obtain an appropriately smoothed cyclic spectrum, these filters must be *phase complementary* in the sense that the phase of the product

$$H_{\Delta f}(\nu + \alpha/2 + f)\, K_{\Delta f}(-\nu + \alpha/2 - f) \quad (47)$$

must be approximately invariant within the passband $\nu \in [-\Delta f/2, \Delta f/2]$. An alternative approach in which the design problem is transferred from phase-complementary filters to phase-locked (in-phase and quadrature) demodulators is described in Section VII.

Case 2: It can be shown that if $H_{\Delta f}$ and $K_{\Delta f}$ are identical LPF's, and if

$$|\alpha| < \Delta f, \quad (48)$$

then (43) reduces to (46a) with $f = 0$ in which

$$S(\alpha, 0) \triangleq 2 \int_{-(\Delta f - |\alpha|)/2}^{(\Delta f - |\alpha|)/2} H_{\Delta f}(\alpha/2 + \nu) \cdot H_{\Delta f}(\alpha/2 - \nu)\, \hat{S}^{\alpha}_{x}(\nu)\, d\nu\, G^{\alpha}_{1/\Delta t}(\alpha). \quad (46c)$$

Thus, an envelope detector at the output of an LPF-(square-law)-BPF device yields the magnitude of the spectrally smoothed cyclic spectrum (46c) as depicted in Fig. 1(e). But to obtain an appropriately smoothed cyclic spectrum, the LPF $H_{\Delta f}$ must exhibit appropriate phase symmetry about the frequency $\alpha/2$, such that the phase of the product

$$H(\nu + \alpha/2)\, H(-\nu + \alpha/2) \quad (49)$$

is approximately invariant within the passband, $\nu \in [-(\Delta f - |\alpha|)/2, (\Delta f - |\alpha|)/2]$.

VII. Cyclic Demodulation

It follows directly from (17), (14), and (9) (generalized to incorporate an arbitrary data-tapering window) that the temporally smoothed cyclic periodogram of tapered data can be expressed as

$$S^{\alpha}_{x_{1/\Delta f}}(t, f)_{\Delta t} = \Delta f(\{[x(t)\, e^{-i2\pi(\alpha/2 + f)t}] \otimes a_{1/\Delta f}(t)\} \cdot \{[x(t)\, e^{-i2\pi(\alpha/2 - f)t}] \otimes a_{1/\Delta f}(t)\}) \otimes g_{\Delta t}(t). \quad (50)$$

By interpreting $a_{1/\Delta f}$ and $g_{\Delta t}$ as the impulse-response functions of LPF's, the implementation shown in Fig. 2(a), which consists of two demodulation (downconversion) operations followed by a product and an LPF operation, is obtained. By analogy with the term *demodulation* used for conventional spectral analysis ($\alpha = 0$), this method shall be called *cyclic demodulation*.

In order to obtain a real implementation of the cyclic demodulation method, we consider the decomposition of (50) into its real and imaginary parts:

$$[S^{\alpha}_{x_{1/\Delta f}}(t, f)_{\Delta t}]_r = \Delta f(\{(x(t) \cos[2\pi(f + \alpha/2)t]) \otimes a_{1/\Delta f}(t)\} \cdot \{(x(t) \cos[2\pi(f - \alpha/2)t]) \otimes a_{1/\Delta f}(t)\} + \{(x(t) \sin[2\pi(f + \alpha/2)t]) \otimes a_{1/\Delta f}(t)\} \cdot \{(x(t) \sin[2\pi(f - \alpha/2)t]) \otimes a_{1/\Delta f}(t)\}) \otimes g_{\Delta t}(t), \quad (51a)$$

[3]The prime in the notation in (43) indicates that, unlike $S^{\alpha}_{x_{1/\Delta f}}(t, f)_{\Delta t}$, $S^{\alpha}_{x_{1/\Delta f}}(t, f)'_{\Delta t}$ is not necessarily exactly equivalent to a temporally smoothed cyclic periodogram.

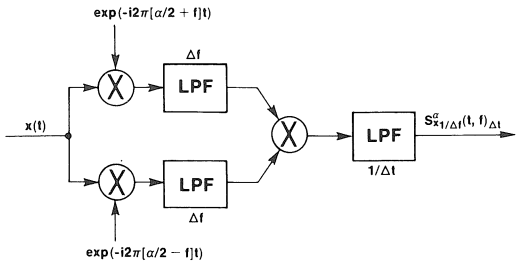

(a)

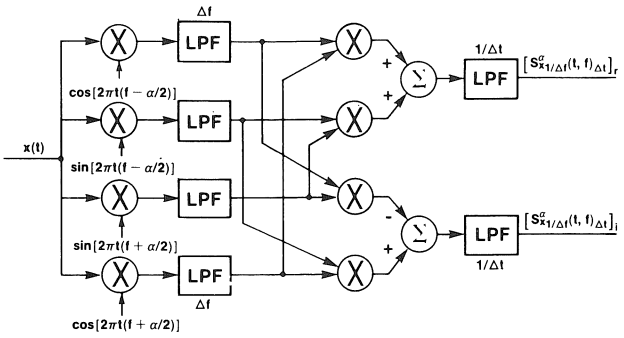

(b)

Fig. 2. (a) Complex demodulation method for cyclic spectral analysis. (b) Real implementation of demodulation method for cyclic spectral analysis.

$$[S^{\alpha}_{x1/\Delta f}(t, f)_{\Delta t}]_i = \Delta f(\{(x(t) \cos [2\pi(f + \alpha/2)t]) \otimes a_{1/\Delta f}(t)\} \cdot \{(x(t) \sin [2\pi(f - \alpha/2)t]) \otimes a_{1/\Delta f}(t)\} - \{(x(t) \sin [2\pi(f + \alpha/2)t]) \otimes a_{1/\Delta f}(t)\} \cdot \{(x(t) \cos [2\pi(f - \alpha/2)t]) \otimes a_{1/\Delta f}(t)\}) \otimes g_{\Delta t}(t). \quad (51b)$$

An implementation of formula (51) is shown in Fig. 2(b). Although quite complicated, in that it requires four phase-locked demodulators, four multipliers, and two LPF's, it is practical for analog implementation.

VIII. Simulations

To illustrate spectral correlation measurement, two cyclostationary signals were simulated, and their spectral correlation functions were measured (computed) using the spectrally smoothed periodogram method (25a), based on an FFT (25b) of a segment of the simulated signal. The two signals are a binary-phased-shift-keyed (BPSK) carrier, with a white binary phase-modulating (data) sequence, and a quarternary-phase-shift-keyed (QPSK) carrier with a white quaternary phase-modulating sequence. It is shown in [1] that for the BPSK signal, the spectral correlation function is given by

$$\hat{S}^{\alpha}_x(f) = \frac{1}{4T_d} \{[Q(f + f_c + \alpha/2)\, Q(f + f_c - \alpha/2) + Q(f - f_c + \alpha/2)\, Q(f - f_c - \alpha/2)]\, e^{-i2\pi\alpha t_o} + Q(f + \alpha/2 + f_c)\, Q(f - \alpha/2 - f_c) \cdot e^{-i(2\pi[\alpha + 2f_c]t_o - 2\phi_o)} + Q(f + \alpha/2 - f_c)\, Q(f - \alpha/2 + f_c) \cdot e^{-i(2\pi[\alpha - 2f_c]t_o - 2\phi_o)}\}, \quad \alpha = k/T_d, \quad (52)$$

for all integers k, where

$$Q(f) = \frac{\sin(\pi f T_d)}{\pi f}, \quad (53)$$

and where f_c and ϕ_o are the carrier frequency and phase, respectively, t_o is the timing parameter for the phase keying, f_d $1/T_d$ is the keying rate, and it is assumed that $2f_cT_d$ is an integer. It is also shown in [1] that for QPSK, the spectral correlation function is given by

$$\hat{S}^{\alpha}_x(f) = \frac{1}{2T_d} [Q(f + \alpha/2 + f_c)\, Q(f - \alpha/2 + f_c) + Q(f + \alpha/2 - f_c)\, Q(f - \alpha/2 - f_c)]\, e^{-i2\pi\alpha t_o}, \quad \alpha = k/T_d, \quad (54)$$

for all integers k. Thus, the only cycle frequencies in both these signals are at harmonics of the keying rate. Hence, an adequate cycle resolution is $\Delta\alpha = 1/10\,T_d$. Also, it follows from (52) and (54) that an adequate spectral resolution is $\Delta f = 1/10\,T_d$. However, because of the reliability condition (24), we must have a cycle resolution width $\Delta\alpha = 1/\Delta t$ that is much smaller than $\Delta f = 1/10\,T_d$.

In Figs. 3 and 4, the magnitude of the measured spectral correlation function is graphed as the height of a surface above the (f, α) plane, for values of f and α available from the FFT of length N. Fig. 3(a) shows the surface for BPSK with a segment length of $N = 128$, a carrier frequency of $f_c = 1/4\,T_s$, a data rate of $f_d = 1/8\,T_s$, and resolutions of $\Delta t = 128\,T_s$ and $\Delta f = 1/32\,T_s$ for a resolution product of $\Delta t\Delta f \cong 4$ (i.e., the number of frequency bins added together by the smoothing operation is $M = 4$). Fig. 3(b) shows a surface for the same signal but with a segment length of $N = 32\,768$, and resolutions of $\Delta t = 32\,768\,T_s$ and $\Delta f = 1/32\,T_s$ for a resolution product of $\Delta t\Delta f \cong 1024$. Fig. 3(c) shows a surface for the same signal, etc., as in Fig. 3(b), except that the signal is embedded in additive Gaussian white noise with total power equal to four times the signal power (SNR $= -6$ dB). It can be seen in Fig. 3(b) that the surface height is nonnegligible for only $\alpha = kf_d$ and $\alpha = \pm 2f_c + kf_d$ for all integers k. It can be seen in Fig. 3(c) that the strong additive noise gives nonnegligible contributions only for $\alpha = 0$, for $\Delta t\Delta f >> 1$. This illustrates the noise-rejection property (for $\alpha \neq 0$) of spectral correlation measurement. Fig. 4(a)–(c) parallels Fig. 3(a)–(c), except that they are for QPSK. Fig. 4(a) [and to a lesser extent Fig. 4(b)] reveals a relatively large variance in the vicinity of $\alpha = \pm 2f_c$ and $f = 0$. This is predicted by the variance formula in Appendix B because $S^0_x(f + \alpha/2)\, S^0_x(f - \alpha/2)$ is large (although $S^{\alpha}_x(f)$ is zero) in this vicinity.

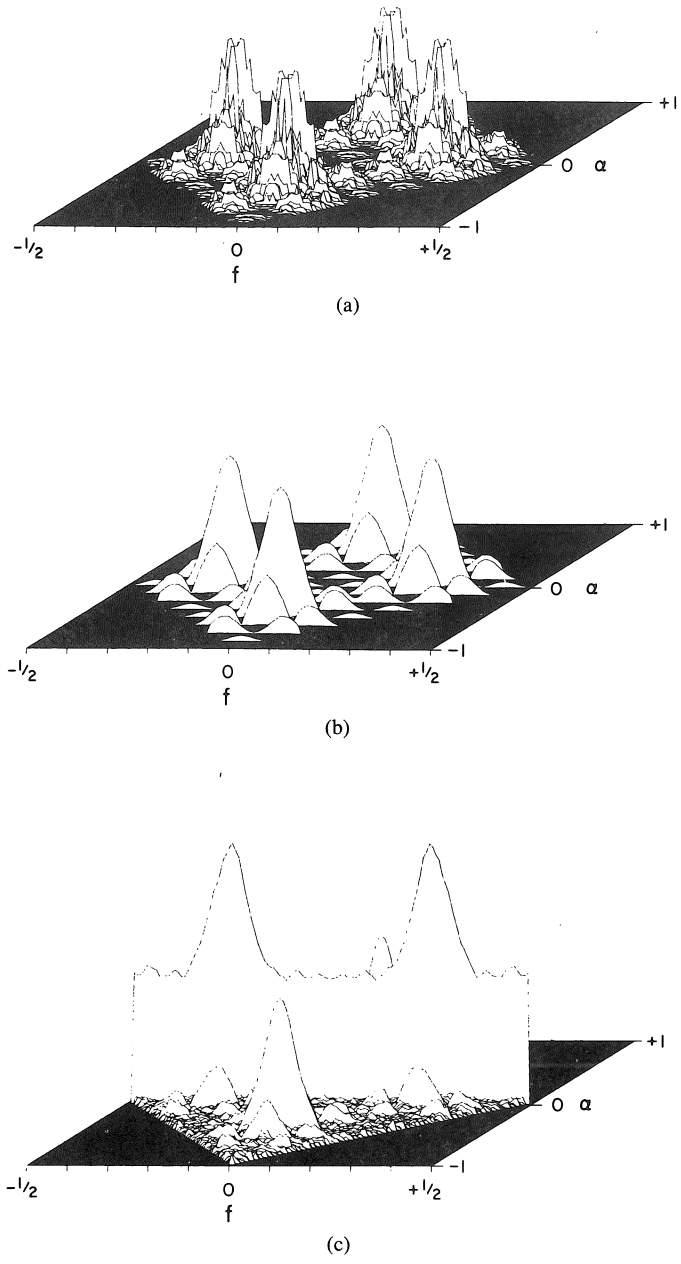

Fig. 3. (a) Measured spectral correlation function magnitude for BPSK with $\Delta t \Delta f \cong 4$. (b) Measured spectral correlation function magnitude for BPSK with $\Delta t \Delta f \cong 1024$. (c) Measured spectral correlation function magnitude for BPSK in noise with SNR $= -6$ dB and $\Delta t \Delta f \cong 1024$.

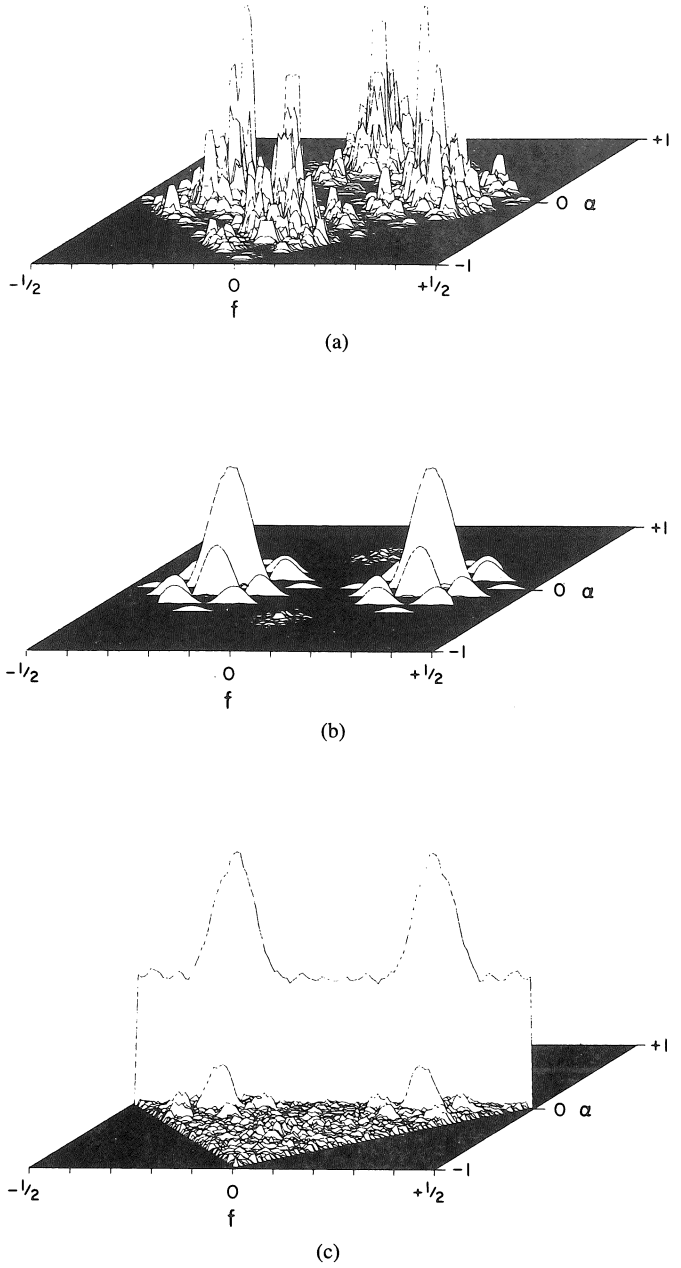

Fig. 4. (a) Measured spectral correlation function magnitude for QPSK with $\Delta t \Delta f \cong 4$. (b) Measured spectral correlation function magnitude for QPSK with $\Delta t \Delta f \cong 1024$. (c) Measured spectral correlation function magnitude for QPSK in noise with SNR $= -6$ dB and $\Delta t \Delta f \cong 1024$.

IX. Conclusion

Various methods for measurement/computation of spectral correlation functions are presented in a unifying theoretical framework. Some of these are amenable to digital hardware or software implementations, others are amenable to analog electrical or optical implementations, and other implementation types used for conventional spectral analysis also are possible. Due to novel problems of computational complexity, cycle phasing, cycle leakage and aliasing, and cycle resolution, the measurement/computation of spectral correlation functions is more challenging than is the measurement/computation of the conventional spectral density function, and also the conventional cross-spectral density function for stationary data. Nevertheless, empirical spectral correlation analysis is indeed practically feasible. The fact that the spectral correlation function for a signal can be accurately measured, even when the signal is buried in noise or masked by interference, contrasts with the fact that noise and interference have an unremovable (in general) masking effect on the measured power spectral density of a signal. This unique noise-rejection and interference-rejection property of spectral correlation measurement has various interesting applications to detection and estimation for signals buried in noise and/or masked by interference (cf. [17] and [18]).

Appendix A
Approximate Equivalence of Temporal and Spectral Smoothing

It is desired to show that the temporally smoothed cyclic periodogram (17) and the spectrally smoothed cyclic periodogram (18) approximate each other for sufficiently large Δt ($\Delta t \gg 1/\Delta f$). For this purpose, let $T = 1/\Delta f$, and consider the string of equalities and one approximation,

$$S^{\alpha}_{x_T}(t, f)_{\Delta t} = \frac{1}{\Delta t} \int_{t-\Delta t/2}^{t+\Delta t/2} S_{x_T}(w, f)\, dw$$

$$= \frac{1}{\Delta t} \int_{t-\Delta t/2}^{t+\Delta t/2} \frac{1}{T} X_T(w, f + \alpha/2) \cdot X_T^*(w, f - \alpha/2)\, dw \quad \text{(A-1)}$$

$$= \frac{1}{T\Delta t} \int_{t-\Delta t/2}^{t+\Delta t/2} \int_{w-T/2}^{w+T/2} x(u)\, e^{-i2\pi(f+\alpha/2)u}\, du \cdot \int_{w-T/2}^{w+T/2} x(v)\, e^{i2\pi(f-\alpha/2)v}\, dv\, dw, \quad \text{(A-2)}$$

$$= \frac{1}{T} \int_{-T/2}^{T/2} \int_{-T/2}^{T/2} \frac{1}{\Delta t} \int_{t+[u+v]/2-\Delta t/2}^{t+[u+v]/2+\Delta t/2} \cdot x(w + [u - v]/2)\, x(w - [u - v]/2) \cdot e^{-i2\pi\alpha w}\, dw\, e^{-i2\pi f(u-v)}\, du\, dv \quad \text{(A-3)}$$

$$\triangleq \frac{1}{T} \int_{-T/2}^{T/2} \int_{-T/2}^{T/2} R^{\alpha}_x(t + [u + v]/2, u - v)_{\Delta t} \cdot e^{-i2\pi f(u-v)}\, du\, dv \quad \text{(A-4)}$$

$$\cong \frac{1}{T} \int_{-T/2}^{T/2} \int_{-T/2}^{T/2} R^{\alpha}_{x_{\Delta t}}(t, u - v) \cdot e^{-i2\pi f(u-v)}\, du\, dv, \qquad \Delta t \gg T \quad \text{(A-5)}$$

$$= \int_{-T}^{T} (1 - |\tau|/T)\, R^{\alpha}_{x_{\Delta t}}(t, \tau)\, e^{-i2\pi f\tau}\, d\tau \quad \text{(A-6)}$$

$$= \int_{-\infty}^{\infty} Tv_T(\tau)\, R^{\alpha}_{x_{\Delta t}}(t, \tau)\, e^{-i2\pi f\tau}\, d\tau \quad \text{(A-7)}$$

$$= \int_{-\infty}^{\infty} z_{1/T}(\nu)\, S^{\alpha}_{x_{\Delta t}}(t, f - \nu)\, d\nu \quad \text{(A-8)}$$

$$= S^{\alpha}_{x_{\Delta t}}(t, f)_{1/T}. \quad \text{(A-9)}$$

In (A-7), v_T is a triangle window with base of length $2T$ and unity area, and in (A-8), $z_{1/T}$ is its scaled Fourier transform, a sinc-squared window with unity area. (If a data-tapering window a_T is used in X_T, then $z_{1/T}$ becomes the squared magntiude of the Fourier tranform $A_{1/T}$.) It follows from the preceding that (with $T = 1/\Delta f$) the approximation

$$S^{\alpha}_{x_{1/\Delta f}}(t, f)_{\Delta t} \cong S^{\alpha}_{x_{\Delta t}}(t, f)_{\Delta f}, \qquad \Delta t \Delta f \gg 1 \quad \text{(A-10)}$$

is close provided that (A-5) is a close approximation. It can be shown that for each T and any $\epsilon > 0$, no matter how small, there exists a Δt sufficiently large ($\Delta t \gg T$, typically) to guarantee that the error of approximation in (A-5) is smaller than ϵ, provided only that the cyclic autocorrelation $\hat{R}^{\alpha}_x$ exists. Thus, the error of approximation in (A-10) is smaller than $\epsilon z_{\Delta f}(f)$ (which is proportional to $1/\Delta f$) for Δt sufficiently large (typically $\Delta t \gg 1/\Delta f$).

In order to determine the cycle resolution capability $\Delta\alpha$ of the temporally smoothed and spectrally smoothed cyclic periodogram, we simply use (A-1)–(A-9) to obtain

$$S^{\alpha}_{x_{\Delta t}}(t, f)_{\Delta f} \cong S^{\alpha}_{x_{1/\Delta f}}(t, f)_{\Delta t} = \int_{-T}^{T} Tv_T(\tau)\, R^{\alpha}_x(t, \tau)_{\Delta t}\, e^{-i2\pi f\tau}\, d\tau, \quad \text{(A-11)}$$

where

$$R^{\alpha}_x(t, \tau)_{\Delta t} \triangleq \frac{1}{\Delta t} \int_{t-\Delta t/2}^{t+\Delta t/2} x(u + \tau/2)\, x(u - \tau/2)\, e^{-i2\pi\alpha u}\, du. \quad \text{(A-12)}$$

It follows from (A-12), as a well-known property of Fourier transformation, that the resolution capability in α of the measurement $R^{\alpha}_x(t, \tau)_{\Delta t}$ is

$$\Delta\alpha = 1/\Delta t, \quad \text{(A-13)}$$

and it follows from (A-11) that this also must be the resolution capability in α of both the measurements $S^{\alpha}_{x_{\Delta t}}(t, f)_{\Delta f}$ and $S^{\alpha}_{x_{1/\Delta f}}(t, f)_{\Delta t}$.

Appendix B
Mean and Variance of Measured Cyclic Spectra

The output of a sliding cyclic spectrum analyzer [e.g., (17) or (18)], tuned to $f = f_o$ and $\alpha = \alpha_o$, can be expressed as

$$z(t) = \int_{-\infty}^{\infty} \int_{-\infty}^{\infty} k(u, v)\, x(t - u)\, x(t - v)\, du\, dv\, e^{-i2\pi\alpha_o t}, \quad \text{(B-1)}$$

in which the kernel is given by

$$k(u, v) = m([u + v]/2, v - u)\, e^{i2\pi f_o(u-v)}\, e^{i\pi\alpha_o(u+v)}, \quad \text{(B-2)}$$

where m is typically of the form

$$m(t, \tau) \cong g_{\Delta t}(t)\, h_{1/\Delta f}(\tau), \quad \text{(B-3)}$$

for which $g_{\Delta t}$ and $h_{1/\Delta f}$ are unimodal[4] windows of widths Δt and $1/\Delta f$, respectively. Approximation (B-3) is either exact or a close approximation at least for $|t| < \Delta t/2$ and $|\tau| < 1/2\Delta f$, provided that $\Delta t \Delta f \gg 1$ (which is generally desired). For example, for the time-smoothed cyclic periodogram method [cf. (50)] using tapered data,

[4]The term *unimodal* is used here to describe windows with a single mainlobe. It does not rule out sidelobes that are small compared to the mainlobe. The unimodality assumption rules out the hopping time-average method since it employs a comb time window $g_{\Delta t}$; also, in this case, (B-3) is not an accurate approximation.

$$h_{1/\Delta f}(\tau) = \int_{-\infty}^{\infty} a_{1/\Delta f}(\tau + t)\, a_{1/\Delta f}(t)\, dt, \qquad \text{(B-4)}$$

where $a_{1/\Delta f}$ is the data-tapering window, and $g_{\Delta t}$ is the time-smoothing window. For the frequency-smoothed cyclic periodogram method [cf. (32)] using tapered data,

$$g_{\Delta t}(t) = |a_{\Delta t}(t)|^2, \qquad \text{(B-5)}$$

where $a_{\Delta t}$ is the data-tapering window, and $h_{1/\Delta f}$ is the inverse Fourier transform of the frequency-smoothing window. Using (B-1)–(B-3), it can be shown [18] that the mean of the analyzer output $z(t)$ is given by

$$\text{mean}\,\{z(t)\} = \sum_{\alpha} m_\alpha\, e^{i2\pi(\alpha - \alpha_o)t}, \qquad \text{(B-6a)}$$

for which

$$m_\alpha \cong G_{1/\Delta t}(\alpha - \alpha_o) \int_{-\infty}^{\infty} H_{\Delta f}(f_o - f)\, \hat{S}_x^\alpha(f)\, df. \qquad \text{(B-6b)}$$

Thus, if there are cycle frequencies α within $\pm 1/2\,\Delta t$ of α_o, or if the sidelobes of $G_{1/\Delta t}$ are not sufficiently small, there can be substantial *cycle leakage* in the analyzer output. Also, if Δf is not small enough to resolve $\hat{S}_x^\alpha(f)$ in f, then there will be a substantial spectral smoothing effect in the output, and if the sidelobes of $H_{\Delta f}$ are not sufficiently small, there can be substantial *spectral leakage*. It follows (as also discussed in Appendix A) that the *cycle resolution* capability of the analyzer is

$$\Delta\alpha^o = 1/\Delta t \qquad \text{(B-7a)}$$

and the *spectral resolution* capability is

$$\Delta f^o = \Delta f. \qquad \text{(B-7b)}$$

When these resolution widths are small enough to resolve $\hat{S}_x^\alpha(f)$, then (B-6b) yields the close approximation

$$\text{mean}\,\{z(t)\} \cong \hat{S}_x^{\alpha_o}(f_o)\, G_{1/\Delta t}(0)\, h_{1/\Delta f}(0). \qquad \text{(B-8)}$$

If it is assumed that the input $x(t)$ to the analyzer is Gaussian (e.g., dominant noise for a low-SNR signal), then it can be shown [18] that the variance (averaged over all time) of the output of the analyzer is given by

$$\text{var}\,\{z(t)\} \cong \frac{\gamma}{\Delta t \Delta f}\,[\hat{S}_x^0(f_o + \alpha_o/2)\, \hat{S}_x^0(f_o - \alpha_o/2) + w_{\Delta f}(2f_o)[\hat{S}_x^0(\alpha_o/2)]^2 + C(f_o, \alpha_o)], \qquad \text{(B-9a)}$$

for which $C(f_o, \alpha_o)$ is a correction term that reflects spectral correlation effects[5]

$$C(f_o, \alpha_o) \triangleq \sum_{\alpha \neq 0} w_{\Delta f}(\alpha)\, \hat{S}_x^\alpha(f_o + \alpha_o/2)\, \hat{S}_x^\alpha(f_o - \alpha_o/2) + \sum_{\alpha \neq 0} w_{\Delta f}(\alpha - 2f_o)\, |\hat{S}_x^\alpha(\alpha_o/2)|^2, \qquad \text{(B-9b)}$$

[5]When two or more uncorrelated spectral components are superposed, their variances add; however, when the spectral components are correlated, the variance of the sum can be either smaller or larger than the sum of variances. This is reflected in the correction term $C(f_o, \alpha_o)$.

where

$$w_{\Delta f}(\alpha) = \frac{\int_{-\infty}^{\infty} H_{\Delta f}(\alpha + f)\, H_{\Delta f}^*(f)\, df}{\int_{-\infty}^{\infty} |H_{\Delta f}(f)|^2\, df} \qquad \text{(B-9c)}$$

$$\gamma = \frac{\Delta t \int_{-\infty}^{\infty} g_{\Delta t}^2(t)\, dt}{\left[\int_{-\infty}^{\infty} g_{\Delta t}(t)\, dt\right]^2} \cdot \frac{\Delta f \int_{-\infty}^{\infty} |H_{\Delta f}(f)|^2\, df}{\left|\int_{-\infty}^{\infty} H_{\Delta f}(f)\, df\right|^2}. \qquad \text{(B-9d)}$$

In (B-9b), it has been assumed that $H_{\Delta f}$ is a real even function, and Δf is small enough to resolve $\hat{S}_x^\alpha(f)$, and that $\Delta t \Delta f \gg 1$; and it has also been assumed that the analyzer exhibits unity gain $G_{1/\Delta t}(0)\, h_{1/\Delta f}(0) = 1$. For typical windows, $g_{\Delta t}$ and $H_{\Delta f}$, γ is on the order of unity. The correction term will be nonnegligible only if there are cycles $\hat{S}_x^\alpha(f) \not\equiv 0$ at values of α within $\pm\Delta f$ of 0 and at values of f within $\pm\Delta f/2$ of $f_o \pm \alpha_o/2$, or at values of α within $\pm\Delta f$ of $2f_o$ and at values of f within $\pm\Delta f/2$ of $\alpha_o/2$. When the correction term in (B-9a) is negligible, and the cycle leakage terms in (B-6b) are negligible, then

$$\frac{|\text{mean}\,\{z(t)\}|^2}{\text{var}\,\{z(t)\}} \cong \frac{\Delta t \Delta f}{\gamma}\, |\hat{C}_x^{\alpha_o}(f_o)|^2, \qquad |f_o| > \Delta f, \qquad \text{(B-10)}$$

where $|\hat{C}_x^\alpha(f)|$ is the autocoherence function [1], [3] defined by

$$\hat{C}_x^\alpha(f) = \frac{\hat{S}_x^\alpha(f)}{[\hat{S}_x^0(f + \alpha/2)\, \hat{S}_x^0(f - \alpha/2)]^{1/2}},$$

which satisfies

$$|\hat{C}_x^\alpha(f)| \leq 1. \qquad \text{(B-12)}$$

Although (B-9) is based on the assumption that $x(t)$ is Gaussian, it is a good approximation for many non-Gaussian signals.

For $x = s + n$ and very low SNR conditions (e.g., in spread-spectrum signal detection), the variance of the output of the analyzer is dominated by the noise at the input. If this noise is stationary with power spectrum $\hat{S}_n^0(f)$, then (B-9) reduces to

$$\text{var}\,\{z(t)\} \cong \frac{\gamma}{\Delta t \Delta f}\,[\hat{S}_n^0(f_o + \alpha_o/2)\, \hat{S}_n^0(f_o - \alpha_o/2)], \qquad |f_o| > \Delta f, \qquad \text{(B-13)}$$

(the variance is doubled for $f_o = 0$). For white noise, $\hat{S}_n(f) = N_o$, (B-13) is simply

$$\text{var}\,\{z(t)\} \cong \frac{\gamma N_o^2}{\Delta t \Delta f}, \qquad |f_o| > \Delta f. \qquad \text{(B-14)}$$

Also, for low SNR, the ratio of squared mean to variance of the analyzer output is, from (B-8) and (B-13),

$$\frac{|\text{mean } \{z(t)\}|^2}{\text{var } \{z(t)\}} \cong \frac{\Delta t \Delta f}{\gamma} \frac{|\hat{S}_s^{\alpha_o}(f_o)|^2}{\hat{S}_n^0(f_o + \alpha_o/2)\, \hat{S}_n^0(f_o - \alpha_o/2)}, \quad |f_o| > \Delta f, \tag{B-15}$$

assuming sufficient spectral and cycle resolution [and a negligible correction term (B-9b)]. On the other hand, if a broad spectral smoothing window is used (as is desired in signal detection applications), then (B-6) and (B-14) yield

$$\frac{|\text{mean } \{z(t)\}|^2}{\text{var } \{z(t)\}} \cong \frac{\Delta t \Delta f}{\tilde{\gamma} N_o^2} \left| \int_{-\infty}^{\infty} H_{\Delta f}(f_o - f)\, \hat{S}_s^{\alpha_o}(f)\, df \right|^2, \tag{B-16}$$

assuming white noise, where $\tilde{\gamma}$ is obtained from γ by replacing the numerator in the second factor in (B-9d) with Δf alone.

Acknowledgment

The author expresses his gratitude to W. A. Brown for his assistance with calculations of the mean and variance of spectral correlation measurements, in Appendix B, and programming for simulations. Thanks are also due B. G. Agee for his assistance with simulations. The interest and support of Dr. C. W. Scott is gratefully acknowledged.

References

[1] W. A. Gardner, *Introduction to Random Processes with Applications to Signals and Systems*. New York: Macmillan, 1986.
[2] R. A. Boyles and W. A. Gardner, "Cycloergodic properties of discrete-parameter nonstationary stochastic processes," *IEEE Trans. Inform. Theory*, vol. IT-29, pp. 105–114, Jan. 1983.
[3] W. A. Gardner, "The spectral correlation theory of cyclostationary time-series," *Signal Processing*, vol. 8, July 1986.
[4] ——, "Structural characterization of locally optimum detectors in terms of locally optimum estimators and correlators," *IEEE Trans. Inform. Theory*, vol. IT-28, pp. 924–932, Nov. 1982.
[5] ——, "The role of spectral correlation in design and performance analysis of synchronizers," *IEEE Trans. Commun.*, to appear.
[6] W. A. Brown, "On the theory of cyclostationary signals," Ph.D. dissertation, Dep. Elec. Comput. Eng., Univ. Calif., Davis, 1986.
[7] T. R. Bader, "Acousto-optic spectrum analysis: A high performance hybrid technique," *Appl. Opt.*, vol. 18, pp. 1668–1672, May 1979.
[8] D. Casasent and B. V. K. Vijaya Kumar, "Optical image plane correlator for ambiguity surface computation," *Appl. Opt.*, vol. 18, pp. 1673–1679, May 1979.
[9] J. D. Cohen, "Ambiguity processor architectures using one-dimensional acousto-optic transducers," in *Proc. SPIE Symp., Real-Time Signal Processing II*, vol. 180, 1979, pp. 134–142.
[10] ——, "Real-time space integrating optical ambiguity processor," in *Proc. SPIE Symp., Real-Time Signal Processing V*, vol. 341, 1982, pp. 148–152.
[11] W. T. Rhodes, "Acousto-optic signal processing: Convolution and correlation," *Proc. IEEE*, vol. 69, pp. 65–79, Jan. 1981.
[12] R. A. K. Said and D. C. Cooper, "Crosspath real-time optical correlator and ambiguity-function processor," *Proc. IEE*, vol. 120, pp. 423–428, Apr. 1973.
[13] P. N. Tamura, J. J. Rebholz, O. T. Daehlin, and T.-C. Lee, "Real-time optical computation of the ambiguity function," in *Proc. SPIE Symp., Real-Time Signal Processing III*, vol. 241, 1980, pp. 104–112.
[14] T M. Turpin, "Spectrum analysis using optical processing," *Proc. IEEE*, vol. 69, pp. 79–92, Jan. 1981.
[15] T. A. C. M. Claasen and W. F. G. Mecklenbräuker, "The Wigner distribution—A tool for time-frequency signal analysis. Parts I–III," *Phillips J. Res.*, vol. 35, pp. 217–250, 276–300, 372–389, 1980.
[16] R. A. Athale, J. N. Lee, E. L. Robinson, and H. H. Szu, "Acousto-optic processors for real-time generation of time-frequency representations," *Opt. Lett.*, vol. 8, pp. 166–168, Mar. 1983.
[17] W. A. Gardner, "Spread-spectrum signal detection: A unifying view," Signal and Image Processing Lab, Dep. Elec. Comput. Eng., Univ. Calif., Davis, Tech. Rep. SIPL-85-6, 1985.
[18] ——, *Statistical Spectral Analysis: A Nonprobabilistic Theory*. Englewood Cliffs, NJ: Prentice-Hall, in press.

William A. Gardner (S'64–M'67–SM'84) was born in Palo Alto, CA, on November 4, 1942. He received the M.S. degree from Stanford University, Stanford, CA, in 1967, and the Ph.D. degree from the University of Massachusetts, Amherst, in 1972, both in electrical engineering.

He was a member of the Technical Staff at Bell Laboratories in Massachusetts from 1967 to 1969. He has been a Faculty member at the University of California, Davis, since 1972, where he is a Professor of Electrical and Computer Engineering. His research interests are in the general area of statistical signal processing, with primary emphasis on the theories of time-series analysis, stochastic processes, and signal detection and estimation. He is the author of *Introduction to Random Processes with Applications to Signals and Systems* (New York: Macmillan, 1986) and *Statistical Spectral Analysis: A Nonprobabilistic Theory* (Englewood Cliffs, NJ: Prentice-Hall, in press).